LATTICE DESIGN FOR POHANG SYNCHROTRON LIGHT SOURCE

K. Nam, J. Choi, S. J. Hahn, S. Oh
PLS Project, Pohang Institute of Science and Technology
P.O.Box 125, Pohang, 790-600 Republic of Korea

For the 2-2.5 GeV Pohang Light Source, a 12 period triple-bend achromat lattice is designed with flat dipole magnets to avoid possible difficulties associated with combined function dipoles. In this arrangement, a quadrupole triplet is introduced per half achromat section for the flexibility in tune and emittance. This lattice configuration yields weak sextupole strengths and shows a good chromatic behaviour in tune versus momentum. An electron beam emittance of $13 \times 10^{-9}\ m \cdot rad$ at 2GeV is achieved with a large dynamic aperture.

Introductory Remarks

The third generation synchrotron light sources are characterized by small horizontal emittance and long straight sections for wigglers and undulators. Triple Bend Achromat(TBA) and Chasman-Green(C-G) lattices are known to be suitable for the requirements of third generation machines. That is, in producing dispersion-free long straight section TBA or C-G lattices give more optimum solution than FODO lattices, but TBA or C-G lattices are rather sensitive to perturbations. For a given circumference, TBA lattices are more eligible than C-G lattices in producing low horizontal emittance and more beam lines, and many on-going projects chose TBA for their storage ring lattices such as LBL ($1.5GeV$), SRRC($1.3GeV$), Super Aco ($0.8GeV$), and Bessy II (1.5-$2GeV$).

Considering these facts, we chose 12 period TBA lattice with flat dipoles for the storage ring of Pohang Light Source. The lattices with combined function dipoles have several advantages over those with flat dipoles such as effective vertical focusing in the dipole magnets and the decrease in the horizontal beam emittance through the increase in the horizontal damping partition number. But, combined function dipoles may cause a serious coupling and, as a result, a shrink in the dynamic aperture. The major storage ring parameters are shown in Table 1.

Lattice Type	TBA
Nominal Energy	2-2.5 GeV
Superperiod	12
Circumference	276.96 m
Mean Radius	44.08 m
Harmonic Number	462
RF Frequency	500.087 MHz
Natural Emittance	13.4 $nm \cdot rad$
Natural Chromaticity (h/v)	-23.1/-17.5
Betatron Tunes (h/v)	14.28/8.18
Beta Functions (h/v)	
Maximum	11.2/21.1 (m)
Minimum	0.97/2.87 (m)
At ID symmetry point	10/4 (m)
Beam Size at ID Symmetry Point	
Horizontal	0.366 (mm)
Vertical (coupling constant $r = 1$)	0.164 (mm)
Maximum Dispersion	0.507 (m)
Momentum Compaction	0.001996
Dipole Length	1.2 (m)
Dipole Field	0.97/1.21 (T)
Length of ID section	6.8 (m)

Table 1. Major storage ring parameters

Magnet Lattice

For the vertical focusing which, otherwise, would be provided by combined function dipoles, we use two defocusing quadrupoles $Q3$, $Q5$ in the achromat section (or dispersive region) as shown in Figure 1. Thus, together with the focusing magnet $Q4$, a triplet of quadrupole magnets is in the half achromat section. But, we use a doublet of quadrupoles in the dispersion-free regions. An alternative arrangement of five quadrupoles is to put a triplet in the dispersion-free region and a doublet in the achromat section as shown in Figure 2.

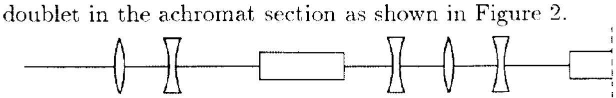

Fig. 1. Two-three arrangement of quadrupoles in the half TBA cell.

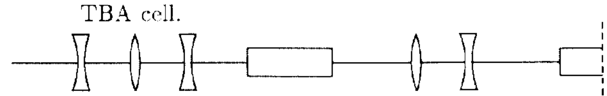

Fig. 2. Three-two arrangement of quadrupoles in the half TBA cell.

The latter configuration (three-two arrangement) looks more familiar than the former one (two-three arrangement). But we chose the former configuration after a comparison study[1,2]. The major advantages of the former configuration are low sextupole strengths and great flexibility in tune and emittance. Specifically, one can summarize the advantages of the two-three arrangement as follows:

1. Depending on the strengths of the quadrupole triplet, the dispersion will vary from zero to a fairly large value in the middle of the center bending magnet. At this time, there is another degree of freedom of controlling horizontal or vertical betatron value at the mirror symmetry point, thus one can detune the system to a large extent from an optimum point through the increase in the dispersion function. Furthermore, due to the flexibility in the phase change across the achromat section, the quadrupole triplet makes it easier to choose the betatron values at the insertion symmetry point independently of the tune of the lattice.
2. The existence of $Q3$ prohibits β_y from growing large so that it contributes to reducing sensitivity and the vertical chromaticity.

A disadvantage of the two-three arrangement is that with a quadrupole doublet in the nondispersive region it is not easy to restore tune shifts and the shrinking in the dynamic aperture caused by disturbances of insertion devices. But in the future we are thinking of adding correction quadrupoles in the up and down stream of insertion devices depending on their strengths and period. Hence, we made a long straight section such as 6.8 m. Magnet lattice parameters are shown in Table 2, and betatron and dispersion functions are shown in Figure 3.

CH2669-0/89/0000-0821$01.00©1989 IEEE

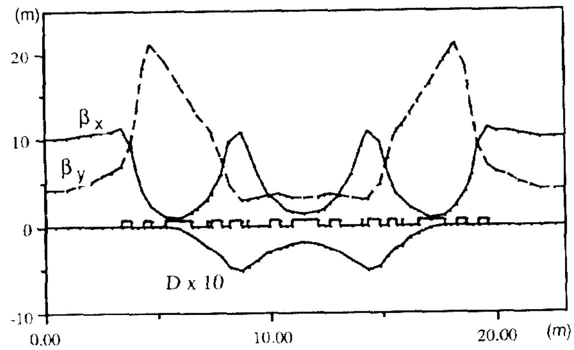

Fig. 3. Lattice functions through one unit cell.

Element	Length (m)	Strength (at 2/2.5GeV)
L0	3.4	
Q1	0.4	9.836/12.295 (Tm^{-1})
L1	0.6	
Q2	0.4	-9.108/-11.385 (Tm^{-1})
L2	0.53	
B	1.2	0.9703/1.213 (T)
L31	0.57	
SD	0.2	-91.9/-114.9 (Tm^{-2})
L32	0.13	
Q3	0.4	-6.987/-8.734 (Tm^{-1})
L4	0.36	
Q4	0.55	11.013/13.766 (Tm^{-1})
L51	0.13	
SF	0.2	60.9/76.1 (Tm^{-2})
L52	0.94	
Q5	0.4	-4.196/-5.245 (Tm^{-1})
L6	0.53	
BH	0.6	0.9703/1.213 (T)

Table 2. Magnet lattice parameters

Chromaticity Correction and Dynamic Aperture

Utilizing one pair of sextupoles (SD, SF) = ($-5.51m^{-2}$, $3.64m^{-2}$) per half lattice, we correct the natural chromaticity (ξ_x, ξ_y) = (-23.08, -17.46) to zero. At this time, we obtain the seemingly flat tune curves versus momentum as shown in Figure 4.

The amplitude dependent tune shifts are obtained such as $\Delta\nu_x = -1040 \cdot 2J_x - 2820 \cdot 2J_y$, $\Delta\nu_y = -2820 \cdot 2J_x - 198 \cdot 2J_y$, where J_x and J_y are the horizontal and vertical action variables. Figure 5 shows the corresponding plots obtained from tracking simulations for 800 turns by utilizing PATRICIA. A comparison of dynamic apertures at ID symmetry point for different tracking codes and tracking turns is shown in Figure 6. In the number of standard deviations (N_x, N_y) the pure horizontal and vertical initial amplitudes are 100 and 140 ($36.6mm$, $23.0mm$).

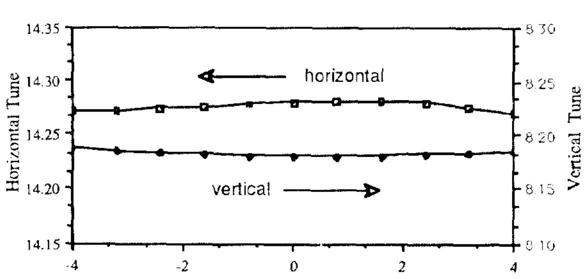

Fig. 4. Betatron tunes versus momentum.

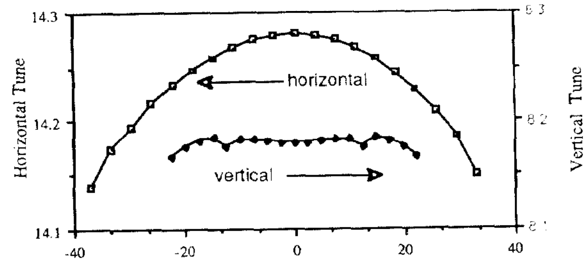

Fig. 5. Horizontal and vertical tunes versus amplitudes.

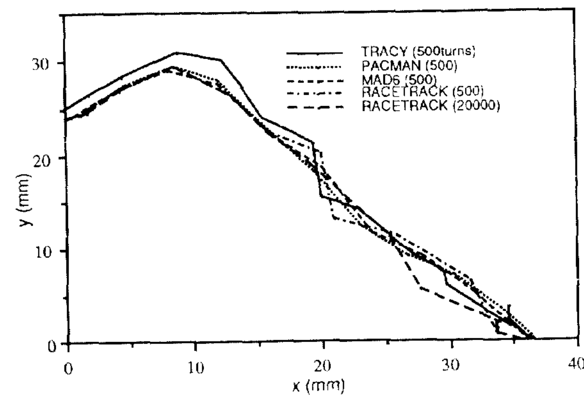

Fig. 6. A comparison of dynamic apertures with different tracking codes and tracking turns.

The fifth order resonance lines $5\nu_x = 12 \cdot 6$, $3\nu_x + 2\nu_y = 12 \cdot 5$, $4\nu_x + \nu_y = 12 \cdot 4$. around the working point (ν_x, ν_y) = (14.28, 8.18) limit the maximum stable ampltitudes, and they are shown as the sharp decreases in the horizontal and vertical dynamic apertures in Figures 7, 8.

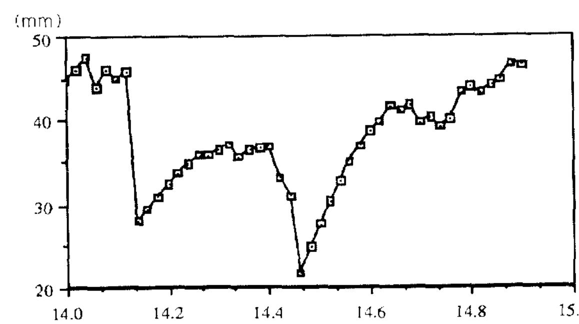

Fig. 7. Horizontal dyanmic aperture for zero coupling versus horizontal tune ($\nu_y = 8.18$).

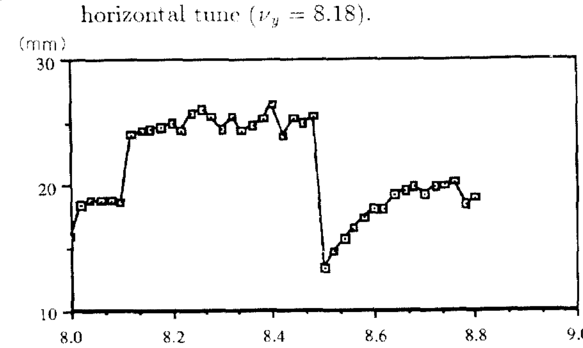

Fig. 8. Vertical dyanmic aperture for full coupling versus vertical tune ($\nu_x = 14.28$).

Multipole Imperfections

In tracking code MAD6, the multipole components are incorporated using a field expansion like

$$B_y(x,\phi) = B\rho \sum_n \frac{k_n x^n}{n!} \cos\{(n+1)\phi + \delta\}$$

where k_n is the multipole amplitude, ϕ is the angle about the beam axis, and δ is an offset angle axis, which measures the skew with respect to the normal orientation. In this case, we use the data in Table 3 which was used in the SRRC lattice design. Here, we have changed the random quadrupole component in the dipole into 10^{-7}, because our dipoles are not combined function dipoles.

	$k_1 l$	$k_2 l$	$k_3 l$	$k_4 l$	$k_5 l$	$k_9 l$
Systematic						
Dipoles	0.0	0.087	0.0	1743	0.0	0.0
Quadrupoles	0.0	0.0	0.0	0.0	$1.5 \cdot 10^5$	$1.5 \cdot 10^{12}$
Random						
Dipoles	10^{-7}	0.174	26.1	174.	0.0	0.0
Quadrupoles	10^{-3}	0.1	15.0	300	$3 \cdot 10^4$	$5 \cdot 10^{11}$

Table 3. Input parameters for multipole error simulations

Figure 9 shows the reduction in the dynamic aperture for 10 different machines when all the systematic and random errors in Table 3 are applied as input for the tracking simulations. A data of one machine was obtained through tracking for 400 turns with MAD6. Figures 10, 11 show the dynamic aperture when only sextupole components in the dipoles and dodecapole components in the quadrupoles of the above errors are applied, respectively.

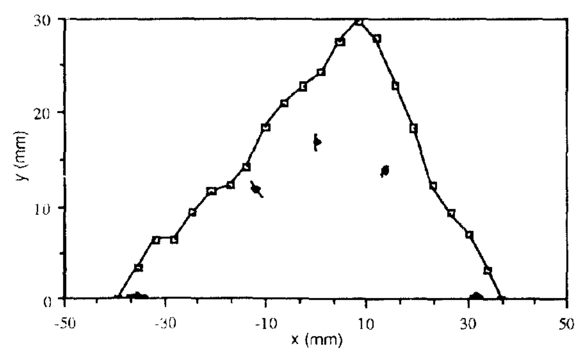

Fig. 9. Dynamic aperture for all systematic and random errors in Table 3. The data points and error bars represent the average dynamic aperture and the rms spread of the dynamic aperture for 10 different machines, respectively.

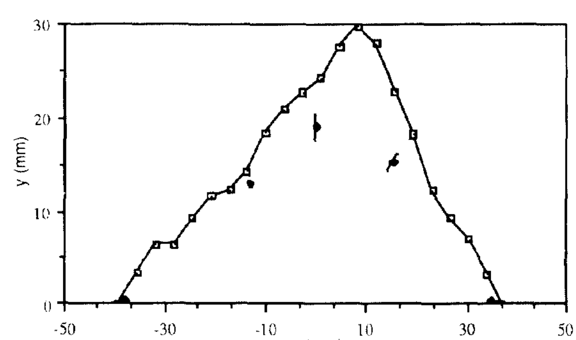

Fig. 10. Dynamic aperture for systematic and random sextupole components in the dipole, $|k_2| = 0.087 m^{-2}$, $(k_2 l)_{rms} = 0.174 m^{-2}$.

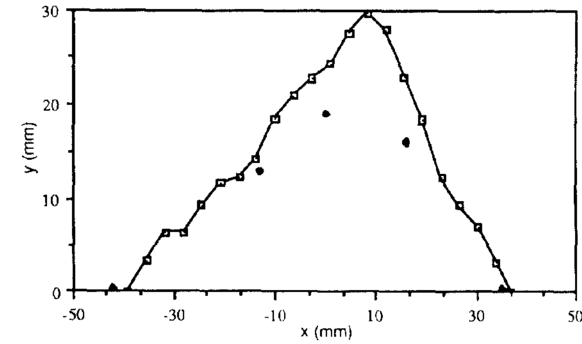

Fig. 11. Dynamic aperture for systematic and random dodecapole components in the quadrupoles, $|k_5 l| = 1.5 \times 10^5$ and $(k_5 l)_{rms} = 3 \times 10^4$.

Flexibility

Combining the strengths of $Q3$, $Q4$ and $Q5$, the dispersion value at the mirror symmetry point can be chosen for a wide range. Also, the tune advance over the achromat section can be manipulated easily, so that β_x and β_y at the ID symmetry point can have, possibly, arbitrary values without changing the tune. Table 4 exemplifies this remark, i.e., it shows the valuse of β_x and β_y at the ID symmetry point for the fixed tune $(\nu_x, \nu_y) = (14.28, 8.18)$. At this time, the sextupole strengths and the maximum betatron values remain low, but the emittance varies to a greater or lesser extent.

Lattice	(β_x, β_y) at ID symm.	Max.(β_x, β_y)	Sextupole strength(m^{-2})	Emittance $(m \cdot rad)$
1	12, 4	13.0, 21.0	−6.1, 4.0	$1.17 \cdot 10^{-8}$
2	10, 4	11.2, 21.1	−5.5, 3.6	$1.34 \cdot 10^{-8}$
3	8, 4	11.0, 21.4	−5.0, 3.3	$1.59 \cdot 10^{-8}$
4	6, 4	11.1, 21.8	−4.6, 3.0	$1.95 \cdot 10^{-8}$
5	4, 4	10.9, 22.6	−4.2, 2.8	$2.50 \cdot 10^{-8}$
6	2, 4	9.1, 24.2	−4.0, 2.8	$3.38 \cdot 10^{-8}$

Table 4. List of various betatron values and other parameters with fixed tune $(\nu_x, \nu_y) = (14.28, 8.18)$.

References

[1] K.Nam, M.Yoon, J.Choi, S.J.Hahn, *Preliminary Lattice Design for Pohang Light Source*, PLS Report, BD 89-01, Jan. 1989.

[2] K.Nam, J.Choi, S.J.Hahn, *Preliminary Lattice Design for Pohang Light Source*, PLS Report, BD 89-03, Feb. 1989.